Research Article

Zahraa M. Nasser, Abdulhaq H. Abedali*, and Hayder A. Alkanaani

Reliability of smart noise pollution map

https://doi.org/10.1515/noise-2022-0167
received January 04, 2023; accepted May 31, 2023

Abstract: The problem of noise pollution in Baghdad, the capital city of Iraq, is getting worse every day as a result of the increased volume of traffic. This presents a considerable risk, particularly on the main roads that connect densely populated neighborhoods such as the Al-Sadr City district with the central neighborhoods of the capital. In order to inform decision-makers in urban development and environmental policy about the high values of noise pollution that require remediation and regulation, noise maps are produced. However, two fundamental problems are generally faced in creating a more reliable noise map in the shortest possible time: the excessive time requirements for measuring noise and determining the method of map creation. Therefore, the role of geographic information system (GIS) software in producing noise maps is evident due to the difficulty of increasing the spatial density of measurements and integrating them with spatial information. Hence, an appropriate interpolation method is required. In this article, Moran's *I* index was calculated to assess the spatial autocorrelation of measured traffic noise points. A comparison was made between the Smart Map Plugin ordinary kriging (OK) and the inverse distance weighting (IDW) deterministic interpolation method to determine the best method for producing noise maps for the main entrance and exit roads of Al-Sadr City. The noise values were modeled using the best-performing method. Furthermore, the predictive raster data are displayed in the spatial context as a starting point and reference for identifying and understanding the levels of traffic noise in the selected study area. The locations of selected points for measuring traffic noise values were determined in an organized and homogeneous manner, where noise points for the main entrance and exit roads were opposite each other, and the distance between consecutive noise points on each road was 100 m. Traffic noise measurements were carried out at each selected point using the SVAN977 sound and vibration analyzer. At each measurement point, three noise values (LAeq, Max, Min) were obtained during the three peak times, 7–9 AM, 12–2 PM, and 4–6 PM. QGIS software was used to compare the two interpolation methods, with its strength lying in the use of plugins that facilitate spatial analysis, processing tools, and algorithms. The Smart Map Plugin provided facilities to choose the appropriate semivariogram in the OK interpolation method. The root mean square error was used to compare the two interpolation methods in order to determine the most suitable method for producing traffic noise maps in the study area. The results indicated that the Smart Map Plugin using OK outperformed the IDW method, as spatial distribution pattern and homogeneity affect the accuracy of interpolation. Moreover, based on the analysis of the three noise attributes (LAeq, Max, Min), the performance of the Smart Map Plugin (OK) was found to be better than IDW when the Moran's *I* value was high.

Keywords: traffic noise, QGIS, Smart Map Plugin, ordinary kriging, IDW

1 Introduction

Traffic on roads is considered one of the most common sources of noise pollution, representing 80% of noise in urban cities [1,2]. Noise pollution has detrimental physiological and psychological effects on human health and well-being [3]. Its effects are often latent but highly harmful, with long-term impacts [4]. Environmental noise pollution is associated with a range of diseases, including tinnitus, cognitive impairment, sleep disturbances, annoyance, as well as cardiovascular diseases that largely result from traffic noise [5–7].

Predicting traffic noise levels on roads is of utmost importance. However, it is a challenging task due to the spatial and temporal correlations of measurement times, and it is critical to accurately determine the spatial interpolation method used to compute high-precision predictions of

*** Corresponding author: Abdulhaq H. Abedali,** Highway and Transportation Department, College of Engineering, Mustansiriyah University, Baghdad, Iraq, e-mail: abdulhaq1969@uomustansiriyah.edu.iq
Zahraa M. Nasser: Surveying Techniques Engineering Department, Technical College, Middle Technical University, Baghdad, Iraq, e-mail: zahraamassernasser193@gmail.com
Hayder A. Alkanaani: Surveying Techniques Engineering Department, Technical College, Middle Technical University, Baghdad, Iraq, e-mail: dr.hayder.a@mtu.edu.iq

the phenomenon under study [8]. Spatial analysts and mapmakers conduct field surveys to measure noise values [9], which are then used to display current traffic noise status and predictors, often using spatial interpolation methods, which means "mapping noise" [10]. In spatial interpolation, the control points are the measured points in the field, which are the representative samples used in interpolation, where the quality of these samples, their spatial distribution, arrangement, and spatial correlation between them, as well as their use for the suitable spatial interpolation, significantly affect the accuracy of the surface produced using prediction tools [11]. For example, noise values are measured at points located on both sides of the main road entering and exiting the city, and researchers are interested in predicting noise levels at each point along this road, where measured noise values depend on several factors, including proximity to the noise-affected area and spatial autocorrelation between measured point values. One of the key steps in modeling traffic noise is to visually represent noise levels using a spatial interpolation method. However, there is still a lack of consensus on the most appropriate interpolation method to match the type and pattern of data distribution under investigation [12]. The most common spatial interpolation techniques are inverse distance weighting (IDW) and ordinary kriging (OK) [13,14]. One widely used approach is kriging, which not only allows for interpolation of unsampled locations but also provides standard errors for the resulting predictions [15]. The geostatistical method of kriging encompasses various types, with one of the most commonly used being OK, which is used in numerous applications including environmental applications, and yields better results when distances along road networks are used [16], especially when the sampling network is evenly distributed [17]. There are two key considerations in the method of kriging: spatial autocorrelation between the measured points and appropriate model selection and fitting for the points. These are fundamental requirements and the main tasks when applying spatial statistics [18]. The kriging technique is suitable for spatial interpolation when the distance between the measured points is spatially related, for example, to explain and determine the spatial variance of traffic noise using kriging. The distance between the measured samples is used to reflect the spatial correlation [19]. The IDW method is one of the most commonly used spatial interpolation techniques which is used as a tool for spatial analysis [20]. The values of unknown points are calculated from the average of known points [21], where the measured noise points are inversely proportional to the distance to the unknown point [22]. IDW is considered most suitable for flat terrain [23] and is primarily used for mapping noise and demonstrating and explaining the reality of noise pollution in the study area [24]. IDW is a powerful and reliable tool for interpolating noise using data obtained from noise sources and the distances between them [25]. When IDW transforms the available spatial data into a continuous spatial surface [26], it provides a visual representation of the areas that are relatively noisy, moderate, and low for the phenomenon under study [27], for evaluating and measuring the spatial and temporal influence of the distribution of traffic noise levels along a major road as an example [28]. In recent years, QGIS has gained numerous users and an active community of developers due to its free and open-source nature, as well as its mastery of functionality [29]. As a result, it has become a serious alternative to commercial geographic information system (GIS) software such as ESRI, with the advantage of being able to access and improve the code. The IDW interpolation tool is available in QGIS software, which is based on GIS [30,31]. Furthermore, QGIS has the advantage of providing us with a plugin that implements specific algorithms using the main program [32]. A plugin called Smart Map has been developed, which is integrated into QGIS version 3.10 or higher, to draw digital maps using interpolation techniques such as OK and machine learning (ML). Python 3.7 was used to develop the software [33]. The graphical user interface (GUI) was designed using PyQt5 and features an easy-to-use interface. As a result, Smart Map has been downloaded more than 15,000 times according to the QGIS plugin repository [33]. The latest version of Smart Map can be found on GitHub and is also available online at https://plugins.qgis.org/plugins/Smart_Map/(accessed on 20 June 2023). A case study was conducted to validate the methodology of OK and ML used in the Smart Map Plugin, where the accuracy of soil attribute interpolation was compared using two different approaches and different sample grids, allowing for the creation of soil attribute interpolation maps [14]. Cross-validation can also be performed by users in the Smart Map Plugin using statistical indicators such as R2 and root mean square error (RMSE) [34]. The aim of this study is to measure and analyze the spatial and temporal variation of traffic noise values measured at selected points on both sides of the main entry and exit roads of the city of Al-Sadr in the Iraqi capital, Baghdad, using Moran's I spatial autocorrelation index. The study also aims to determine the best method for modeling and producing traffic noise maps, by comparing the Smart Map Plugin's OK approach and the deterministic IDW method using the QGIS software.

2 Methodology and material

2.1 Study area

The city of Al-Sadr is located in the northeast of the Iraqi capital, Baghdad, and is a densely populated area with a population of 1,276,249 according to the latest statistics from the Iraqi Ministry of Planning for the year 2020. Al-Sadr city is connected to the center of Baghdad province by four main roads. To study traffic noise in Al-Sadr city, the most important of these main roads was selected. The study area included the two main roads for entering and leaving Al-Sadr city, which extend from Al-Muthaffar Square to Market Maridi, round-trip during the morning and afternoon periods. The study area included Al-Muthaffar street and Al-Jawader street as shown in Figure 1. As for the evening period, the study area included the two main roads from Al-Muthaffar Square to the intersection of Zayn al Qaws Street and Al-Jawader Street, because the road leading to Maridi market is closed at night and only allows pedestrian traffic. The two main roads selected for the study for entering and exiting Al-Sadr are busy and vibrant roads bordered by residential areas, parks, commercial and service areas, as well as government and industrial institutions. The transportation system in Al-Sadr relies on small buses, private transport vehicles, motorcycles, as well as tik tok (three-wheeled vehicles) that are widely spread throughout the city.

2.2 Noise survey, processing data, and creating spatial database

First, the methodology of the study included a field survey of noise levels. After conducting a field reconnaissance of

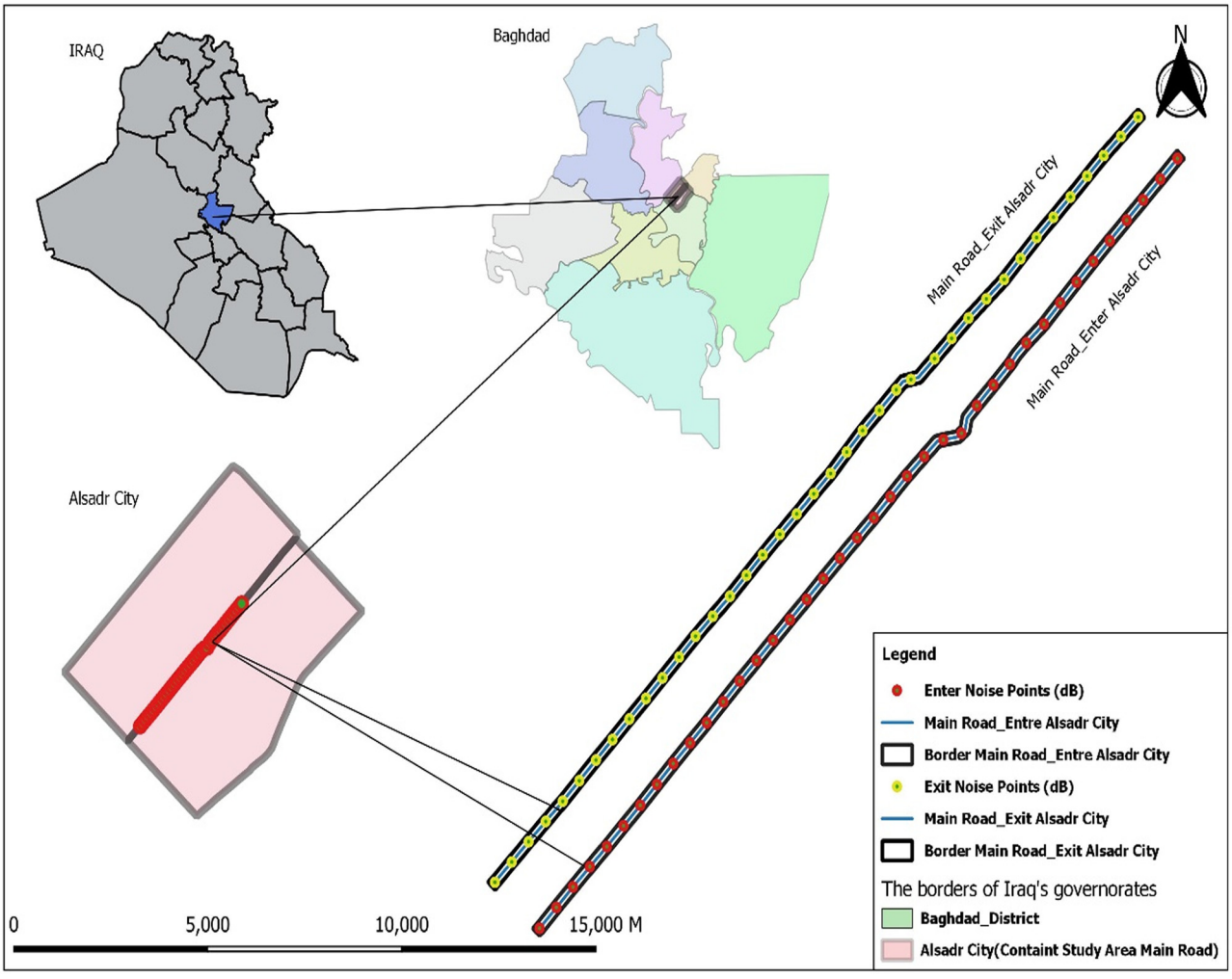

Figure 1: The study area's geographical location and the measured noise point distribution for the main road to enter and exit from Al-Sadr city, Baghdad, Iraq.

the main road leading in and out of the city of Al-Sadr, selected points were identified for measuring traffic noise levels. The measured traffic noise points on both entry and exit roads were opposite each other, and the distance between every two successive noise points on each road was 100 m, measured using a measuring tape. The spatial coordinates of each measured noise point were determined using Garmin GPS Map 64s. The noise levels were measured using a SVAN977 sound and vibration analyzer with an A-type filter, and the measurement duration at each point was 5 min. The device was installed at a distance of 1 m from the sidewalk, with a height of 1.5 m above the ground and a detector precision of 0.1 dB. Eighty points of traffic noise were measured for both the entry and exit roads of Al-Sadr city. Measurements were taken for each point during three periods: morning (7–9 am), midday (12–2 pm), and evening (4–6 pm). At each measurement point, three noise values (LAeq, Max, Min) were obtained. The statistical results, including the mean, standard deviation, minimum value, and maximum value, for the measured noise points for both the entry and exit roads of Al-Sadr city and for the three measurement periods, are presented in Tables 1 and 2. The environmental conditions for noise measurements were represented by a dry road surface, with the ambient air temperature within the moderate continental range, where the temperature did not fall below 5°C or exceed 35°C, and the wind speed did not exceed an average of 10 m/s. Second, the methodology of the study involved downloading field measured data and processing it using the software platform SvanPC++, where the extracted data included noise values (LAeq, Max, Min) for each measured traffic noise point. The data were exported from platform SvanPC++ to an Excel file that included the spatial coordinates of each measured noise point. Third, a spatial geodatabase was created using version 3.22 of the QGIS software, and processing was performed within the program to create feature class layers for the measured noise points for the main entry and exit roads, as well as for the three measurement periods.

2.3 Smart Map Plugin (OK)

The Smart Map Plugin is a software component developed and integrated with QGIS version 3.10 or higher [33]. The interpolation is performed using the Smart Map Plugin (OK) through an open-source Python library called PyKrige, which supports the 2D OK technique and includes variogram models [35]. The Smart Map Plugin simplifies the process of digital map drawing using OK interpolation without the need for programming knowledge [33]. Furthermore, it facilitates the examination of variations and the implementation of interpolation using the significant parameters of the OK method, such as the number of neighbors, search radius, semi-variogram, and its factors (range, sill, nugget, and fitting the mathematical models) [33,36]. The developed Smart Map Plugin (OK) was used to configure a suitable statistical semi-variogram for performing the interpolation, where the plugin allows the user to fit five models of the theoretical semi-variogram: exponential, spherical, Gaussian, linear, and linear with sill. The cross-validation method was used to choose the semi-variogram model. The search radius for kriging was set equal to the range obtained by the semi-variogram. The number of neighbors for the main entrances and exits during morning and afternoon periods were determined as 25 points, while for the evening period, the number of neighbors was set to 20 points. The maps produced by the plugin are exported to QGIS in raster format. In addition to that, Figure 2a represents the interface of the Smart Map plugin for selecting and entering the measured layers and Figure 2b includes the facilities provided by the plugin for selecting the appropriate semi-variogram.

Table 1: Descriptive statistics for the measured noise points of the main road of entry to Al-Sadr City (for the period from January 30 to February 3, 2022)

Measurement time	Noise value (dB)	Mean	Standard deviation	Minimum value	Maximum value
Morning	LAeq	73.3642	2.31442	70	78.536
Noon	LAeq	75.1641	2.20762	70.598	79.308
Evening	LAeq	75.3193	2.20906	68.874	78.66
Morning	Max	87.3968	2.6043	82.756	93.478
Noon	Max	89.4801	2.3202	84.46	93.647
Evening	Max	88.7003	2.80681	79.06	92.624
Morning	Min	63.1884	3.39804	53.306	68.944
Noon	Min	65.2585	2.95761	58.24	69.602
Evening	Min	66.9153	2.3573	62.19	71.472

Table 2: Descriptive statistics for the measured noise points of the main road of exit from Al-Sadr City (for the period from January 30 to February 3, 2022)

Measurement time	Noise value (dB)	Mean	Standard deviation	Minimum value	Maximum value
Morning	LAeq	72.8247	2.0646	68.24	76.688
Noon	LAeq	73.4312	1.9831	69.146	77.484
Evening	LAeq	75.2294	1.93787	70.326	79.002
Morning	Max	86.4943	2.08927	81.984	90.444
Noon	Max	87.286	2.43432	82.86	91.936
Evening	Max	89.1617	2.21231	83.922	93.41
Morning	Min	63.3783	3.02103	56.544	68.63
Noon	Min	61.8386	4.87014	54.042	70.826
Evening	Min	66.5087	2.31909	60.91	70.978

2.4 Moran's *I* (index)

Moran's *I* is a commonly used measure for assessing spatial autocorrelation and is also a useful indicator for analyzing spatial association of environmental variables [14]. It is available in the Smart Map Plugin of the QGIS software, where the spatial weight matrix (W) for Moran's *I* is calculated in Smart Map using the PySAL Python library. The PySAL library provides a kernel function that determines weights for neighbors based on distances between sample points in the grid. The univariate Moran's *I* is used to measure, compare, and test the degree of autocorrelation of the same variable that is interpolated at different distances. Therefore, the spatial autocorrelation degree was calculated for traffic noise attributes (LAeq, Max, Min) for three measurement periods in the morning, afternoon, and evening using Moran's *I*, as shown in Figure 3. The mathematical formula for calculating the value of Moran's *I* (Legendre & Fortin, 1989) is as follows:

$$I = \frac{N\sum_{i=1}^{n}\sum_{j=1}^{n}W_{ij}(X_i - X^{-})(X_j - X^{-})}{\sum_{i=1}^{n}\sum_{j=1}^{n}W_{ij}\sum_{i=1}^{n}(X_i - X^{-})^2}, \quad (1)$$

where N is the number of observations, $\bar{x}$ is the mean of the variable, X_i is the variable value at a particular location, X_j is the variable value at another location, W_{ij} is a weight indexing location of i relative to j, in the smart map plugin, and (W) represents the spatial weight matrix, the sum of all w_{ij}.

When the value of univariate Moran's *I* is zero, it indicates that the variable under study shows no spatial correlation and that the pattern is random. When the value of Moran's *I* is closer to −1, it indicates that the variable tends to have more contrasting values, and as its value approaches 1, it indicates that the variable tends to have higher similarity values and that the pattern is clustered rather than random.

2.5 Generation scenarios for evaluating the interpolation methods

A comparison was conducted between the Smart Map Plugin (OK) and the IDW method to determine which method is better for producing traffic noise maps for the study area. The noise level value of LAeq was used as the interpolation attribute, representing the equivalent sound pressure level in decibels, and yielding a high level of Moran's *I* during the three measurement periods. The comparison was performed by drawing an equal number of measured traffic noise points, located in the same spatial location for each interpolation method, with 18 points for both the main entry and exit roads of Al-Sadr city considered as check points. These points were represented as a feature class in the project's geodatabase. While the remaining traffic noise points, which are also represented as a feature class in the project's Geodatabase, have the same spatial location in both of the interpolation methods and consist of 62 points for the two main entry and exit roads of Al-Sadr city, they are used to perform interpolation in both comparison methods. Regarding the traffic noise points selected to check the interpolation methods, they were identified using the random selection algorithm that deals with vector data. The number of selected features method within the random selection algorithm was chosen to select the number of points to be drawn for the purpose of checking, and this method helped identify the nature of the check sample distribution. To have complete control over the checking process, some adjustments were made manually by the user in the point selection process. The noise points selected for check and evaluating the noise models were located in opposite directions of each other. The points for the entry road were located in the opposite direction of the exit road, and vice versa. Additionally, the check points were chosen in an organized

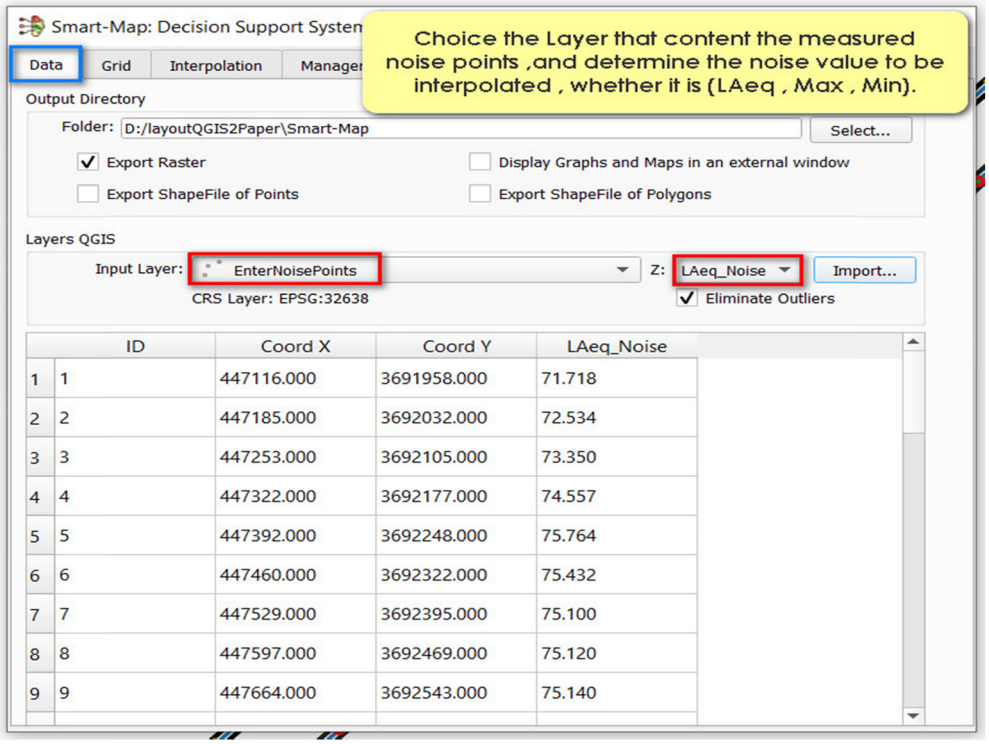

(a)

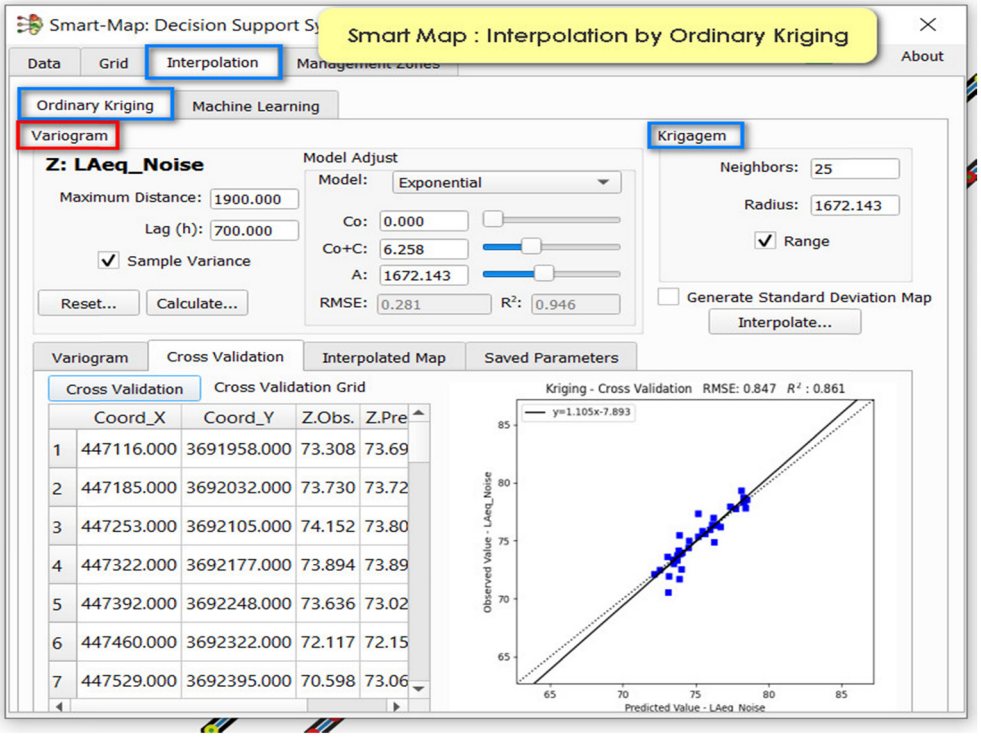

(b)

Figure 2: Graphical User Interface for Smart Map. (a) Selection the traffic noise data value to be interpolated. (b) Determine the parameters and configuration semi-variograms for the Ordinary kriging interpolation method.

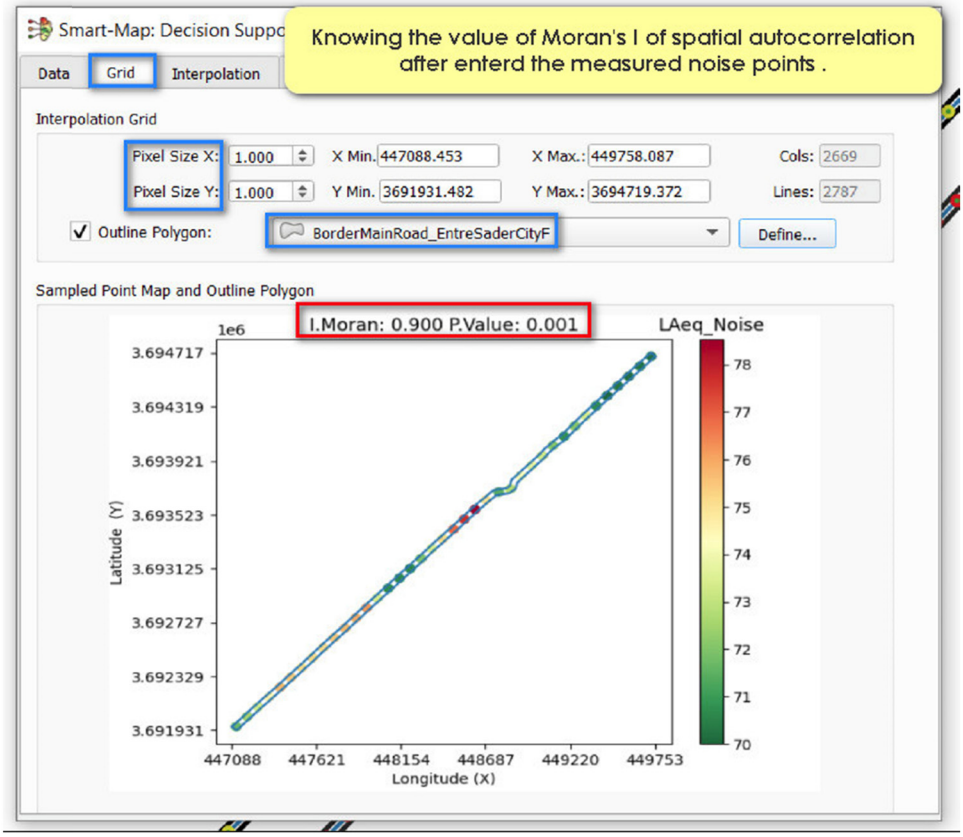

Figure 3: GUI of Smart Map. Moran's *I* calculation of the spatial autocorrelation between noise points measured, for the entre main road at morning in Al-Sadr City using LAeq noise value.

manner, as illustrated in Figure 4. The identified traffic noise points for the examination process were exported to a new feature class within the project's Geodatabase for use in comparing two interpolation methods. The remaining traffic noise points were utilized for the interpolation process using both the Smart Map Plugin (OK) and IDW methods, with each method producing a raster with the same number of points and for three measurement periods as shown in Figures 5 and 6. During the comparison between the two interpolation methods, the fundamental parameters for each method were determined. For the Smart Map Plugin (OK) method, the primary parameters were identified, represented by the search radius equal to the range, as well as the number of neighbors and the semi-variogram configuration. In the IDW method, the main parameters are represented by the distance coefficient *P*, in addition to defining the extent of the predicted raster layer. The resulting raster is then clipped along the boundaries of the study area. In both methods, the pixel size of the resulting raster is set to 1 m × 1 m. To evaluate and validate the spatial interpolation quality in the Smart Map Plugin (OK) and IDW methods, selected check points are used, in addition to the raster resulting from the interpolation of the remaining noisy points. First, it is verified whether the predictive raster resulting from the interpolation using both methods has been properly generated. This is done by using the raster pixel to point algorithm to convert the predictive raster to points, to ensure that individual pixel units within the raster do not contain null values in the output results. Then, the check points and raster resulting from the remaining traffic noise points are entered into the sample raster value logarithm to extract the values of the selected check points within the predictive raster and create a new vector layer. The new vector layer created by the sample raster value algorithm has the same properties as the input data, with knowledge of the corresponding raster values for the location of the specified check point. The logarithmic field calculator and its associated expression are used to create an error field and calculate its value by subtracting the interpolated value from the measured value of the specified check points. The mean prediction error is then calculated through the statistics panel available in the QGIS software. Finally, the logarithmic field calculator and its associated expression are used again to square the error value to find the RMSE value, which is calculated according to Eq. (2).

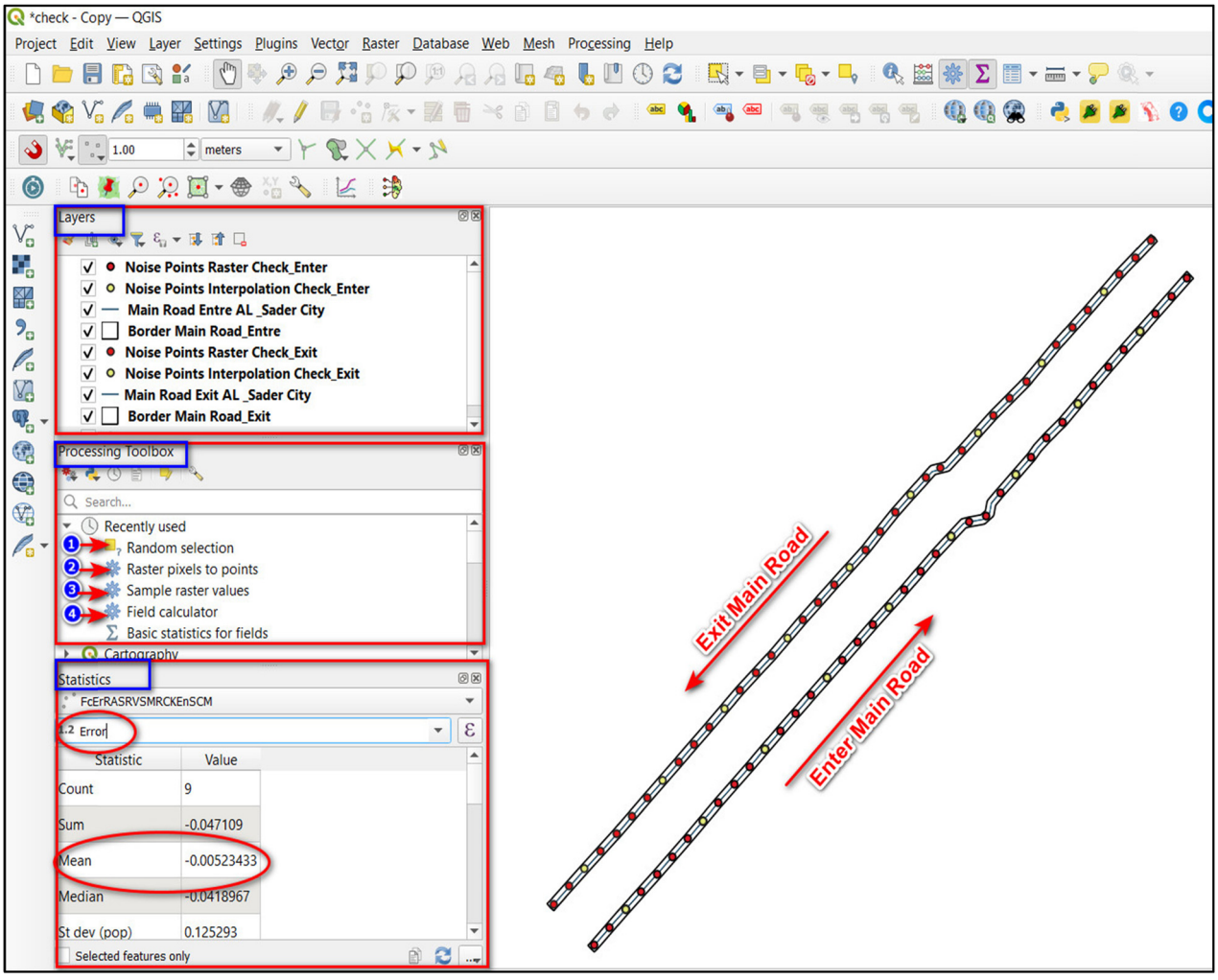

Figure 4: The interface of the QGIS program and the algorithms used for the purpose of performing the validation to compare the raster generated by both methods, IDW and Smart Map Plugin (OK), using check points.

Using this value, the best method for producing traffic noise maps for the entry and exit roads of Sadr City can be determined.

$$\text{RMSE} = \sqrt{\frac{1}{n}\sum_{i=1}^{n}(x_i - \hat{x}_i)^2}, \tag{2}$$

where $\hat{x}_i$ represents the interpolated value of the noise attribute at point i, x_i is the observed value of the traffic noise attribute at point i, and n is the number of points.

In addition, Figure 7 briefly illustrates the methodology used in this study.

3 Interpolation methods used in noise mapping

One of the key considerations in producing noise maps is the use of spatial interpolation techniques to interpolate spatial data for unsampled points based on their proximity to sampled points [1]. In these methods, a continuous raster surface of estimated values is produced using the information at the sampled point locations [37]. There are two main types of interpolation methods: deterministic methods that produce estimations without evaluating interpolation errors [38] and statistical methods that produce estimations with evaluated interpolation errors, *i.e.*, uncertainty, which are represented as estimated variances and are associated with the interpolated values [39,40]. The IDW and OK methods are among the univariate interpolation methods, where only the primary variable samples are used in the interpolation process [41]. Additionally, interpolated values are displayed in a regular grid pattern, which is smoother than the area used for sampling [42,43]. Interpolation methods are used to produce raster surfaces at a spatial resolution determined by the user [44].

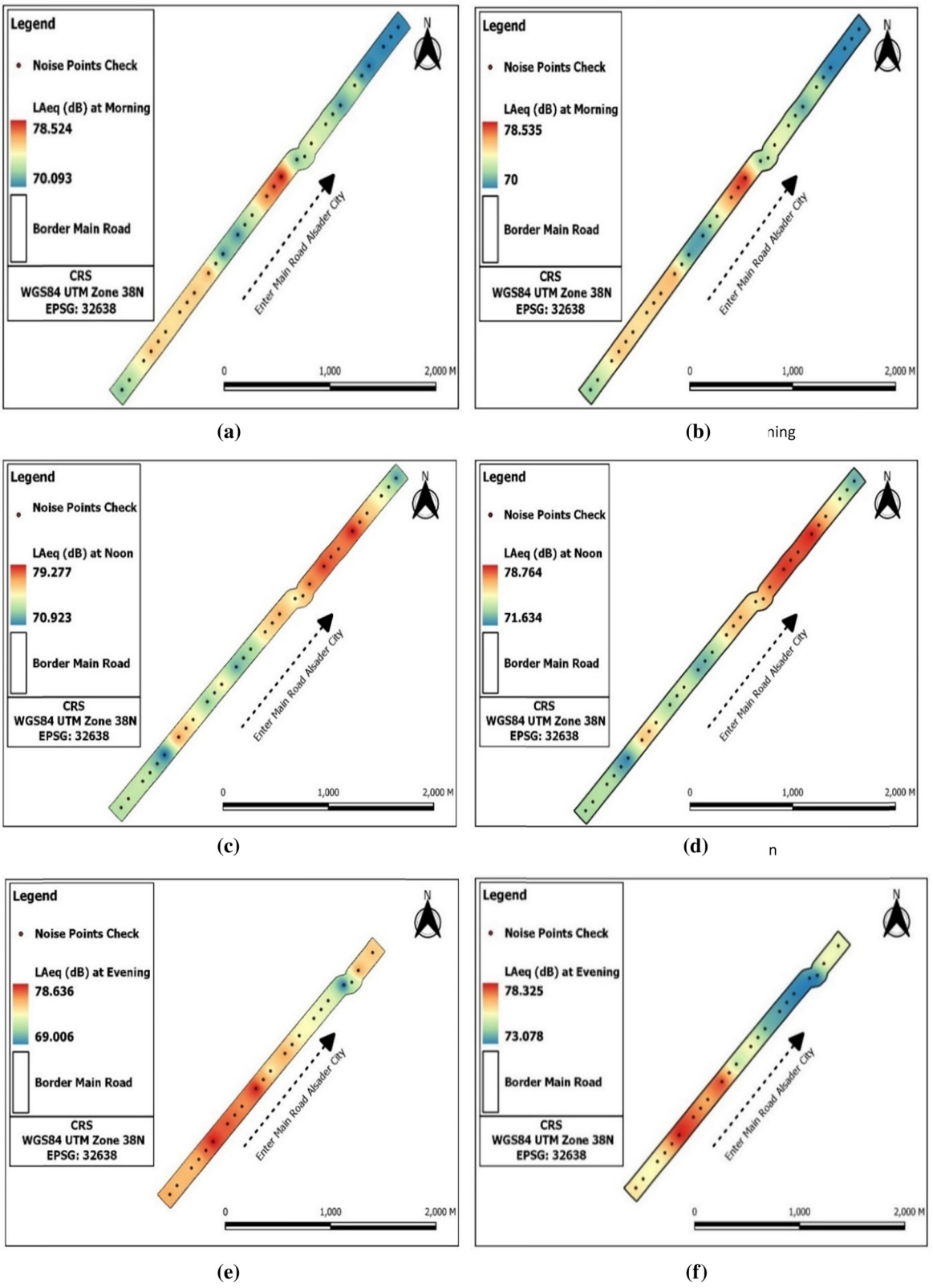

Figure 5: Comparison between the Smart Map Plugin (OK) and the IDW method, using the LAeq noise value, for three periods, morning, noon, and evening, for the main entry road to Al-Sadr City. (a) IDW method morning, (b) Smart Map (OK) method morning, (c) IDW method noon, (d) Smart Map (OK) method noon, (e) IDW method evening, and (f) Smart Map (OK) method evening.

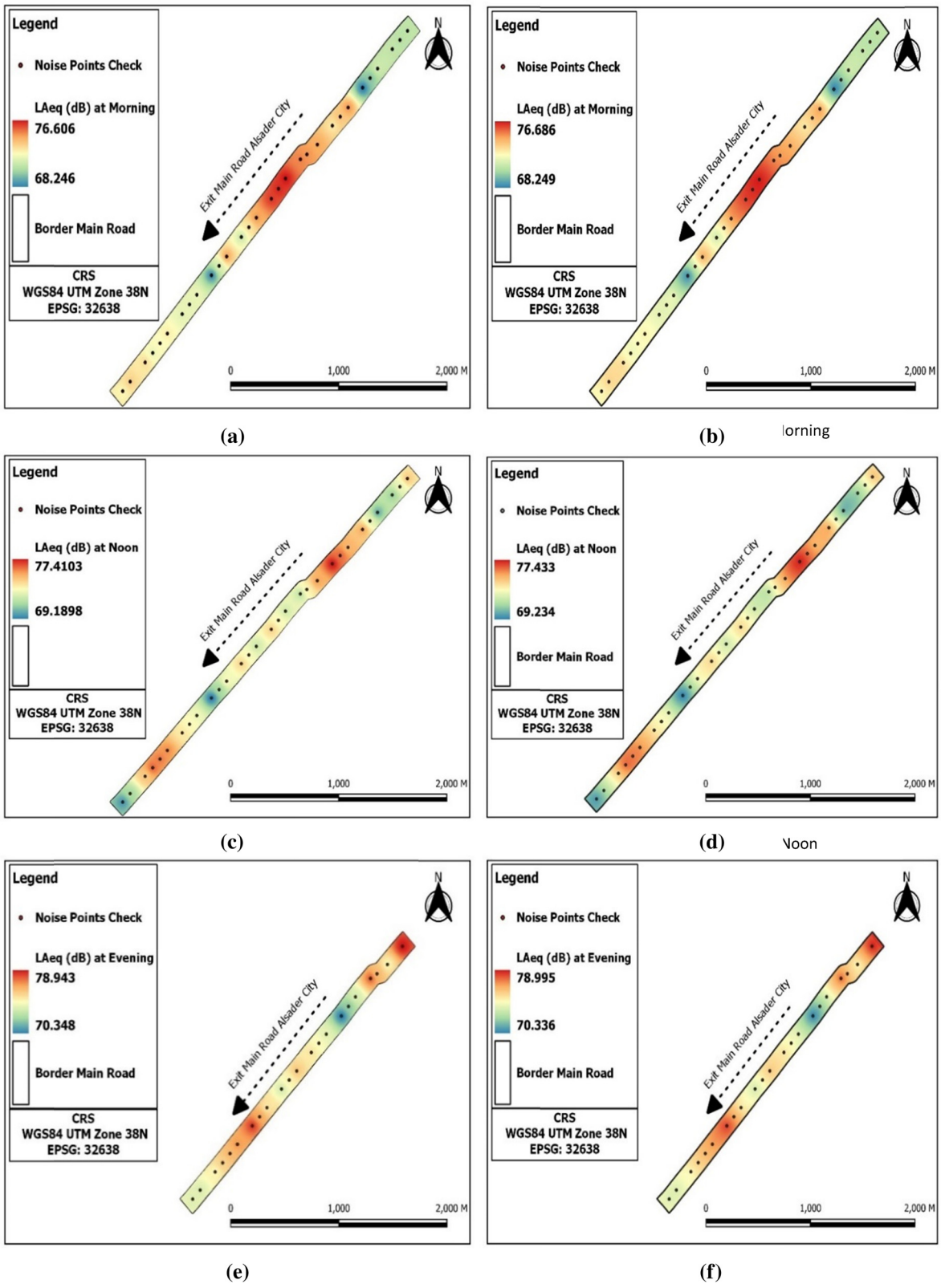

Figure 6: Comparison between the Smart Map Plugin (OK) and the IDW method, using the (LAeq) noise value, for three periods, morning, noon, and evening, for the main exit road to Al-Sadr City. (a) IDW method morning, (b) Smart Map (OK) method morning, (c) IDW method noon, (d) Smart Map (OK) method noon, (e) IDW method evening, and (f) Smart Map (OK) method evening.

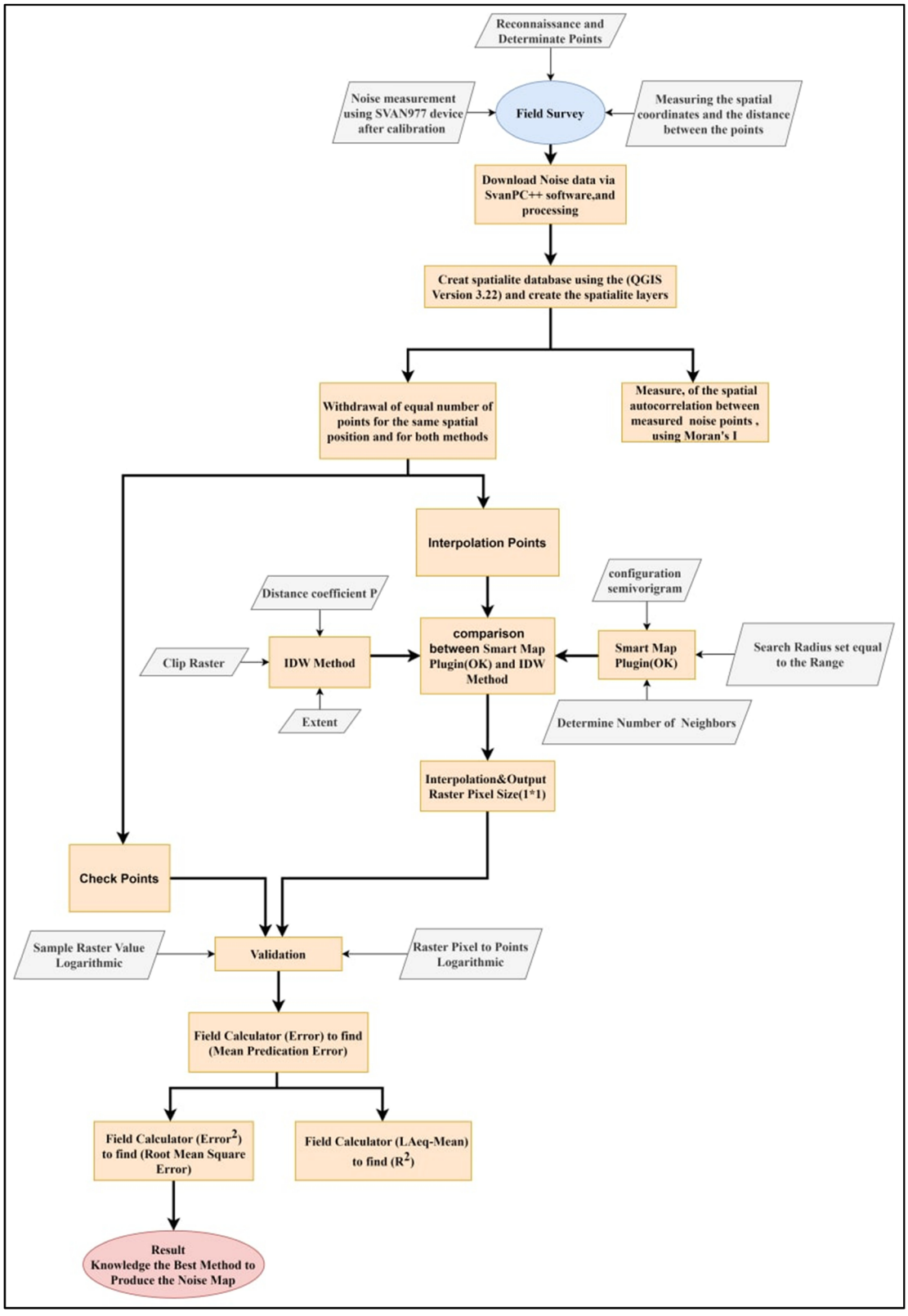

Figure 7: Study methodology.

3.1 Interpolation by IDW method

IDW is a spatial interpolation method used to generate an overlay raster surface using the Z value of point attributes with known spatial coordinates [43]. Each cell derived using this method takes into account a distance factor, connecting the closest measured points, and estimates values between them [42,45]. This method is referred to as "inverse distance weighted" because the unknown point is influenced by all measured points, but the impact is greater when the distance between the unknown and known point is small, and decreases as the distance increases [46,47]. When the distance between the unknown point and each known point is weighted, the average weight of the measuring point is calculated, but this is not a direct increase in weight, rather an inverse increase, *i.*e., the weight is inverse [48]. In its simplest form, IDW is referred to as "linear interpolation," where weights are calculated using the linear function of the distance between measured points and the interpolate point [43]. It is one of the deterministic methods based on the following mathematical law [38]:

$$\hat{Z}(s_0) = \sum_{i=1}^{N} \lambda_i Z(s_i), \tag{3}$$

where $\hat{Z}(s_0)$ is the predictive value, N is the number of samples points measured and will be used in prediction, λ_i is the measured point weight, and $Z(s_i)$ is the observed value.

$$\lambda_i = d_{i0}^{-p} / \sum_{i=1}^{N} d_{i0}^{-p}, \tag{4}$$

where the weight is reduced by the p coefficient when the distance is large and d_{i0} represents the distance between each measured point s_i and the prediction site s_o.

Interpolation is performed using the IDW method in the QGIS software by inputting the measured noise point layer and selecting the interpolation attribute field, which represents noise values (Min, Max, LAeq). The parameter of the distance coefficient weight was set to 2, and the pixel size of the resulting raster was adjusted to 1 × 1. The raster is created on the extent of the study area, and then a clip is made to create the raster on the boundaries of the main road for entry and exit from the city of Sadr. The raster is then classified and the interpolated noise values are displayed within the selected study area boundaries.

3.2 Interpolation by OK method

It is an advanced spatial statistical method [49]. It is a well interpolator that produces an estimator surface (raster) from a set of discrete measured points with Z values and uses kriging to verify the spatial behavior of the studied phenomenon [42]. The Kriging method is similar to the IDW method, where non-measured locations are interpolated by weighting the distance to surrounding measured points. However, the difference is that Kriging method not only relies on distance, but also on the arrangement of measured points and spatial autocorrelation [14,43,49]. In the Kriging method, there are statistical and mathematical steps, where the kriging algorithm requires a positivity spatial autocorrelation model, and the semi-variogram plot describes this relationship between measured samples of the studied phenomenon [49,46,43,42]. This statistical model is used to find mathematical functions of variables and an interpolation surface that is sought after [42,49]. However, appropriate mathematical models for the data must be selected, and there must be positivity during modeling to show and describe spatial continuity [43,49]. Among many unbiased estimates, Kriging is considered the "best linear unbiased estimator" (used in statistics to estimate random effects in linear mixed models) [46]. Kriging results indicate that interpolation takes into account gradual spatial changes, and predictions do not pass through known measured points but rather predict higher and lower values than the original measured values [43,44]. The most common and widely used method belonging to the Kriging family is OK, a flexible and simple univariate local method [42,46]. It estimates the local mean, *i.e.*, the sample mean within the search window, and requires homogeneity and spatial autocorrelation among the measured samples [46]. OK uses the appropriate semi-variogram program to calculate interpolation weights, and the semi-variance is linked to the distance between measured sample points [49]. OK allows for transformations, removal of external directional bias from resulting statistical layers, and measurement of prediction errors [38]. The general equation for OK is as follows [38]:

$$Z(s) = \mu + \varepsilon(s), \tag{5}$$

where s is a location (X, Y), $Z(s)$ is the measured value at that location, μ is the mean for data (no trend) on which the model is based, and $\varepsilon(s)$ is random errors. The predictor is formed as a weighted sum of the data.

$$\hat{Z}(s_0) = \sum_{i=1}^{N} \lambda_i Z(s_i), \tag{6}$$

where $\hat{Z}(s_0)$ is the predicted value at that location, s_0 is the prediction location, and λ_i is an unknown weight for the measured value.

4 Results and discussions

4.1 Spatial autocorrelation with Moran's *I*

The spatial autocorrelation of traffic noise values (LAeq, Max, Min) measured along the two main roads entering and leaving the city of Al-Sadr was examined using Moran's *I* for three measurement periods: morning, afternoon, and evening. The correlation analysis was conducted on a sample of traffic noise points measured along the main entrance and exit roads of the city, ranging from 5 to 40 points. Moran's *I* was used to assess the degree to which traffic noise values were spatially clustered along the main roads. It was observed that Moran's *I* tend to increase as the number of measured traffic noise points along the main roads increases. The average value of Moran's *I* for the measured traffic noise values was calculated for the two main roads entering and exiting the city, and is depicted in black for the three measurement periods in Figure 8.

Figure 8a and b depicts the spatial autocorrelation between traffic noise points measured on the main entrance and exit roads of Al-Sadr city during the morning rush hour. A weak autocorrelation was observed at a sample size of 5, which increases with an increasing number of points until it stabilizes at a high level. The values of Moran's *I* for the traffic noise values (LAeq, Max, Min) on the main entrance road were 0.9, 0.893, and 0.828, respectively, while those for the main exit road were 0.888, 0.835, and 0.920, respectively. The Moran's *I* value for the Min values on the entrance road in the morning was slightly lower than that for the LAeq and Max noise values. On the other hand, the Moran's *I* value for the Max noise values on the exit road in the morning was slightly lower than that for the LAeq and Min noise values. It should also be noted that the Moran's *I* values for the Max and LAeq noise values for the main entrance road in the morning and for the Min noise value for the main exit road in the morning were higher than the average Moran's *I*.

In Figure 8c and d, which represents the spatial autocorrelation between traffic noise points measured for the main entrance and exit roads of Sadr city at noon, strong spatial autocorrelation was observed from the beginning for the LAeq and Min noise values, where Moran's *I* was constant and stable for both roads, with values of 0.898 and 0.918 for the entrance road, and 0.883 and 0.947 for the exit road, respectively. However, the Moran's *I* value for the max noise value decreased at the sample size of 5, then gradually increased to reach a stable value of 0.733 for the entrance road and 0.838 for the exit road, which is lower compared to the Moran's *I* value for the LAeq and Min noise values. In addition, Moran's *I* for noise values LAeq and Min appears to be higher than the average Moran's *I*.

In addition, in Figure 8e and f, which represents the spatial autocorrelation between traffic noise measurements for the main entrance and exit roads of Al-Sadr city in the evening, Moran's *I* values for LAeq noise levels show high correlation values until reaching a stable value of 0.886 for the entrance road, while showing initially moderate values for the exit road before increasing and continuing in this upward trend until reaching a stable value of 0.879. The values of Max traffic noise in the evening exhibit a high and stable spatial autocorrelation, which stabilizes with a Moran's *I* value of 0.860 for the entrance road and 0.883 for the exit road. Additionally, the Min traffic noise values in the evening exhibit a low Moran's *I* value at a sample size of 5, then begin to increase and stabilize at a value of 0.874 for the main entrance road and a value of 0.903 for the main exit road, which is higher than its value for LAeq and Max noise levels for the exit road in the evening. It is also noteworthy that the Moran's *I* value for LAeq noise values for the entrance road in the evening was higher and very close to the average Moran's *I*, while the Moran's *I* value for the Min noise values for the exit road in the evening was higher than the average Moran's *I*.

The decrease in Moran's *I* is attributed to the variation among some of the measured traffic noise points value, which slightly reduces the spatial correlation between the samples. According to the spatial analysis of the areas surrounding the main entrance and exit roads of Al-Sadr City, the variation in some values of the traffic noise is a result of differences in traffic congestion in some parts of the studied main roads (Table 3).

4.2 Comparison between IDW and Smart Map (OK) methods

A comparison was made between the Smart Map Plugin (OK) method and the IDW method using the LAeq value for measured traffic noise points during three measurement periods in the morning, afternoon, and evening. Several processing steps were performed within the QGIS software to evaluate the interpolation methods. The comparison between the interpolation methods was conducted under similar conditions, using parameters that provided the best results for each method. The results of the comparison and check between the two interpolation methods showed that the Smart Map Plugin (OK) method outperformed the IDW method, as it gave the lowest standard deviation and

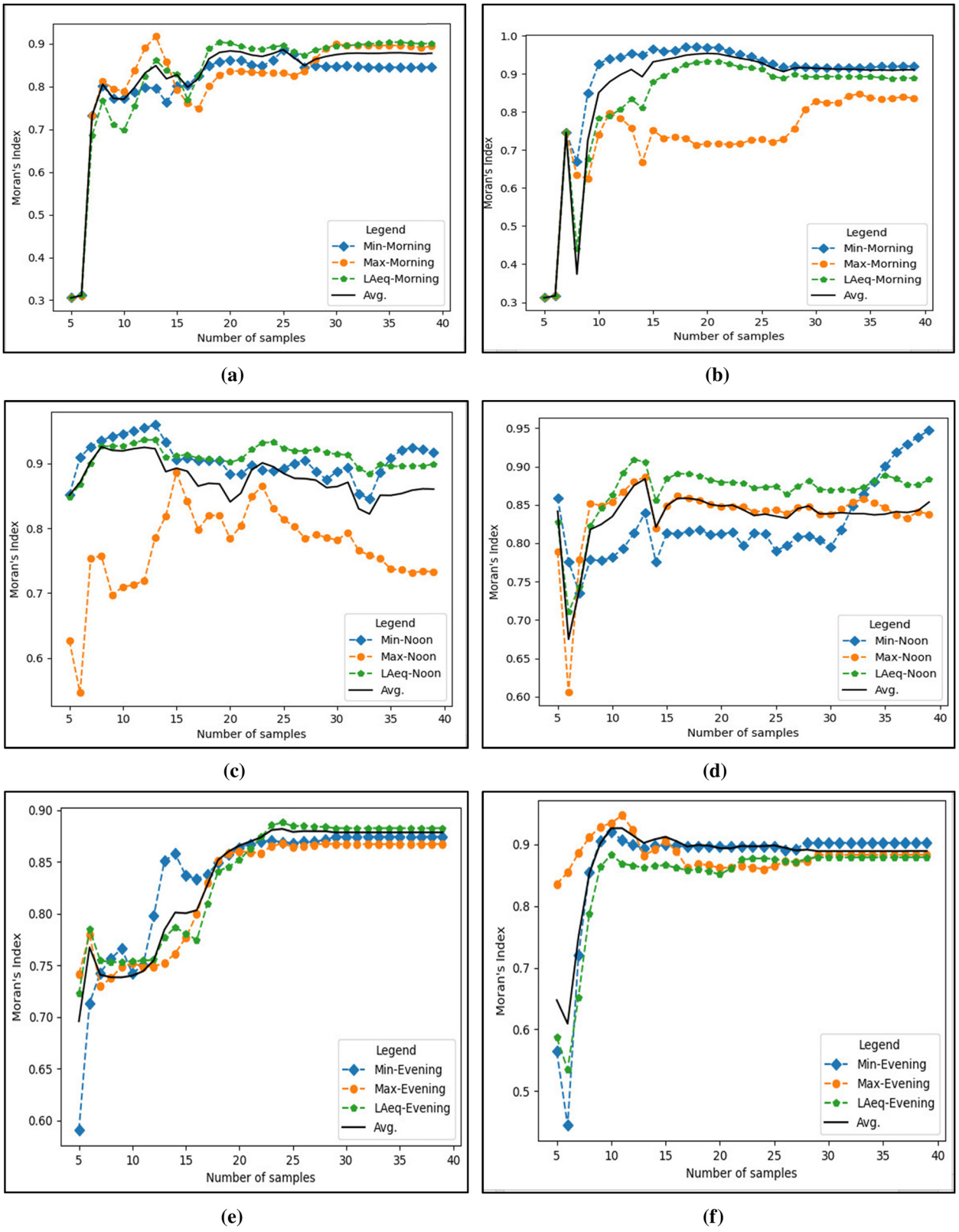

Figure 8: Computing Moran's *I* for the spatial autocorrelation, between the measured traffic noise points, for the (LAeq), (Max), and (Min) values and measuring the average Moran's *I*. (a) Morning enter, (b) Morning exit, (c) Noon enter, (d) Noon exit, (e) Evening enter, and (f) Evening exit.

Table 3: Values of Moran's *I* and pseudo *p*-value calculated for each set of samples chosen before and after the check procedure, for the two main roads to enter and exit AL-Sadr City, for three measurement periods, and three traffic noise attributes

Attribute	39 samples for the road to enter in the morning		30 samples for the road to enter in the morning	
	Moran's *I*	*p*-value	Moran's *I*	*p*-value
LAeq	0.9	0.001	0.814	0.001
Max	0.893	0.001	0.797	0.001
Min	0.828	0.001	0.654	0.011
Attribute	**39 samples for the road to enter in the noon**		**30 samples for the road to enter in the noon**	
	Moran's *I*	*p*-value	Moran's *I*	*p*-value
LAeq	0.898	0.001	0.820	0.001
Max	0.733	0.001	0.588	0.036
Min	0.918	0.001	0.886	0.001
Attribute	**29 samples for the road to enter in the evening**		**22 samples for the road to enter in the evening**	
	Moran's *I*	*p*-value	Moran's *I*	*p*-value
LAeq	0.886	0.001	0.726	0.009
Max	0.860	0.001	0.725	0.002
Min	0.874	0.001	0.728	0.003
Attribute	**39 samples for the road to exit in the morning**		**30 samples for the road to exit in the morning**	
	Moran's *I*	*p*-value	Moran's *I*	*p*-value
LAeq	0.888	0.001	0.777	0.001
Max	0.835	0.001	0.682	0.005
Min	0.920	0.001	0.841	0.001
Attribute	**39 samples for the road to exit in the noon**		**30 samples for the road to exit in the noon**	
	Moran's *I*	*p*-value	Moran's *I*	*p*-value
LAeq	0.883	0.001	0.738	0.001
Max	0.838	0.001	0.590	0.036
Min	0.947	0.001	0.877	0.001
Attribute	**29 samples for the road to exit in the evening**		**22 samples for the road to exit in the evening**	
	Moran's *I*	*p*-value	Moran's *I*	*p*-value
LAeq	0.879	0.001	0.708	0.002
Max	0.883	0.001	0.711	0.003
Min	0.903	0.001	0.766	0.001

RMSE. Additionally, the statistical results of the comparison and check showed that the mean prediction error obtained using the Smart Map Plugin (OK) method was lower than that obtained using the IDW method for the main entrance and exit roads of Al-Sadr city and for the three measurement periods. Except for the evening exit road, the mean prediction error resulting from using IDW was lower due to the decrease in Moran's *I* value resulting from the decrease in spatial correlation between traffic noise points. When using the Smart Map Plugin (OK) and inputting all measured traffic noise points, the value of Moran's *I* is high. However, it is noted that this value decreases after selecting a portion of the points for examination, as shown in Table 3. The statistical results of comparing the Smart Map Plugin (OK) method and the IDW method were displayed using Data Plotly (a plugin in QGIS that allows for creating graphs using Plotly library and Python API), as illustrated in Figures 9 and 10.

4.3 Interpolated maps

The three noise attributes (LAeq, Max, Min) were interpolated for all measured traffic noise points on the main entry and exit roads of Al-Sadr City. The Smart Map Plugin (OK) was used for interpolating the traffic noise attributes, as shown in Figures 11–13, because it gave the lowest RMSE values for the three measurement periods, namely, morning, afternoon, and evening after comparing it with the IDW method. Grids with cell sizes of 1 m × 1 m were used. After the spatial interpolation process, areas of high and low noise levels were found along the surface of the main entry and exit roads of Al-Sadr City. Regarding the predictive maps that were created for the purpose of comparison and validation between the Smart Map plugin (OK) method and the IDW method, using the noise level value (LAeq) as the *Z* value, there was a noticeable difference between the spatial patterns of the maps produced by each interpolation method. The spatial distribution and arrangement of the data, as well as the spatial correlation between them, along with the quality of the data, can affect the performance of the spatial interpolation method and the accuracy of the resulting surface. This may be the reason why the OK method advanced with caution. Furthermore, the transitions between LAeq values were smoother in the prediction maps produced using OK.

5 Conclusions

The land surrounding the main entry and exit roads of Al-Sadr city included residential, commercial, and service areas, industrial zones, public buildings, and recreational areas. According to the Iraqi Noise Control Law of 2015, the

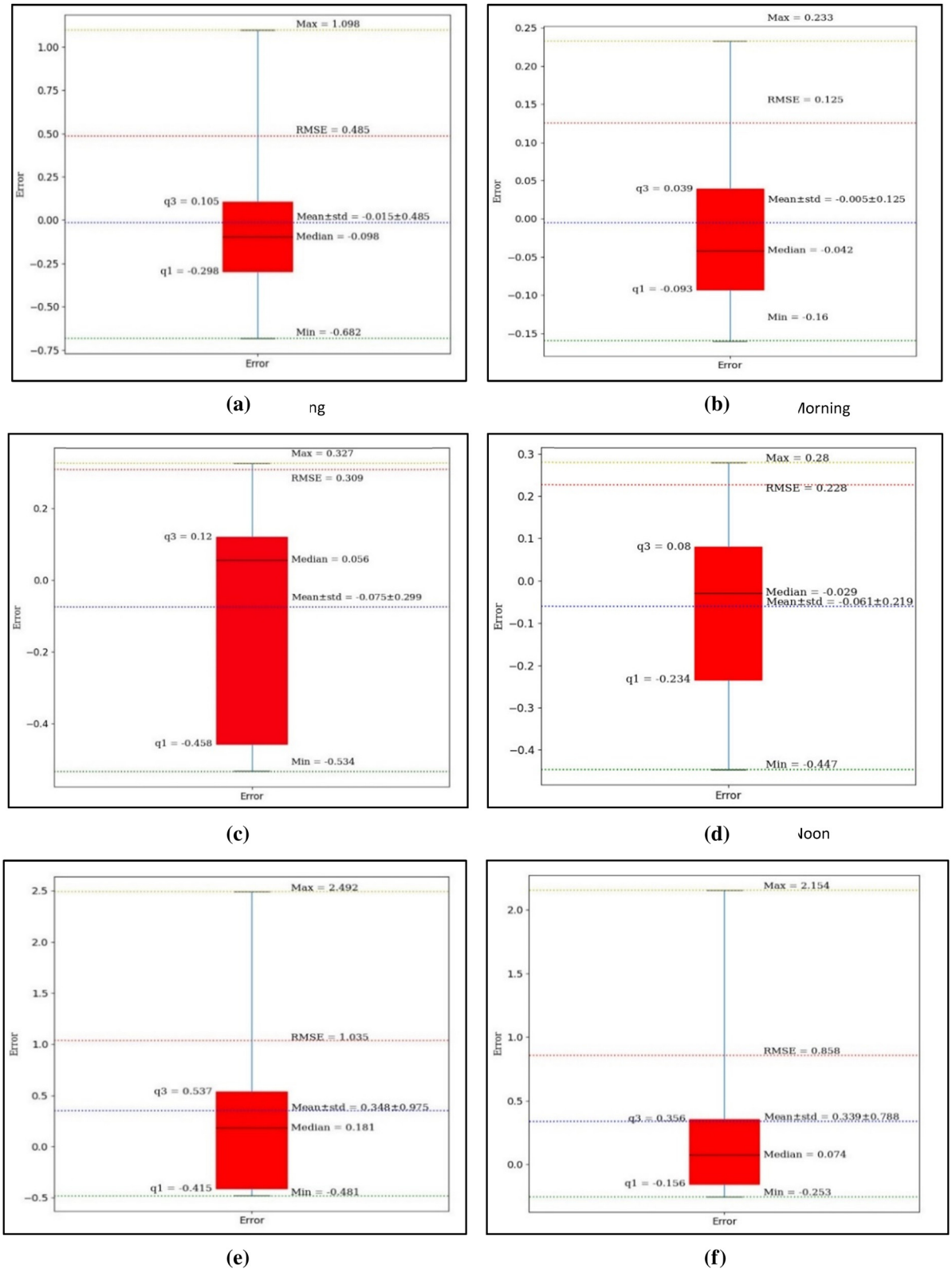

Figure 9: The statistical results of the check process using the Smart Map Plugin (OK) method and the IDW method, for the main road to enter Al-Sadr City, and for three measurement periods, morning, noon, and evening. (a) Check IDW morning, (b) Check Smart Map (OK) morning, (c) Check IDW noon, (d) Check Smart Map (OK) noon, (e) Check IDW evening, and (f) Check Smart Map (OK) evening.

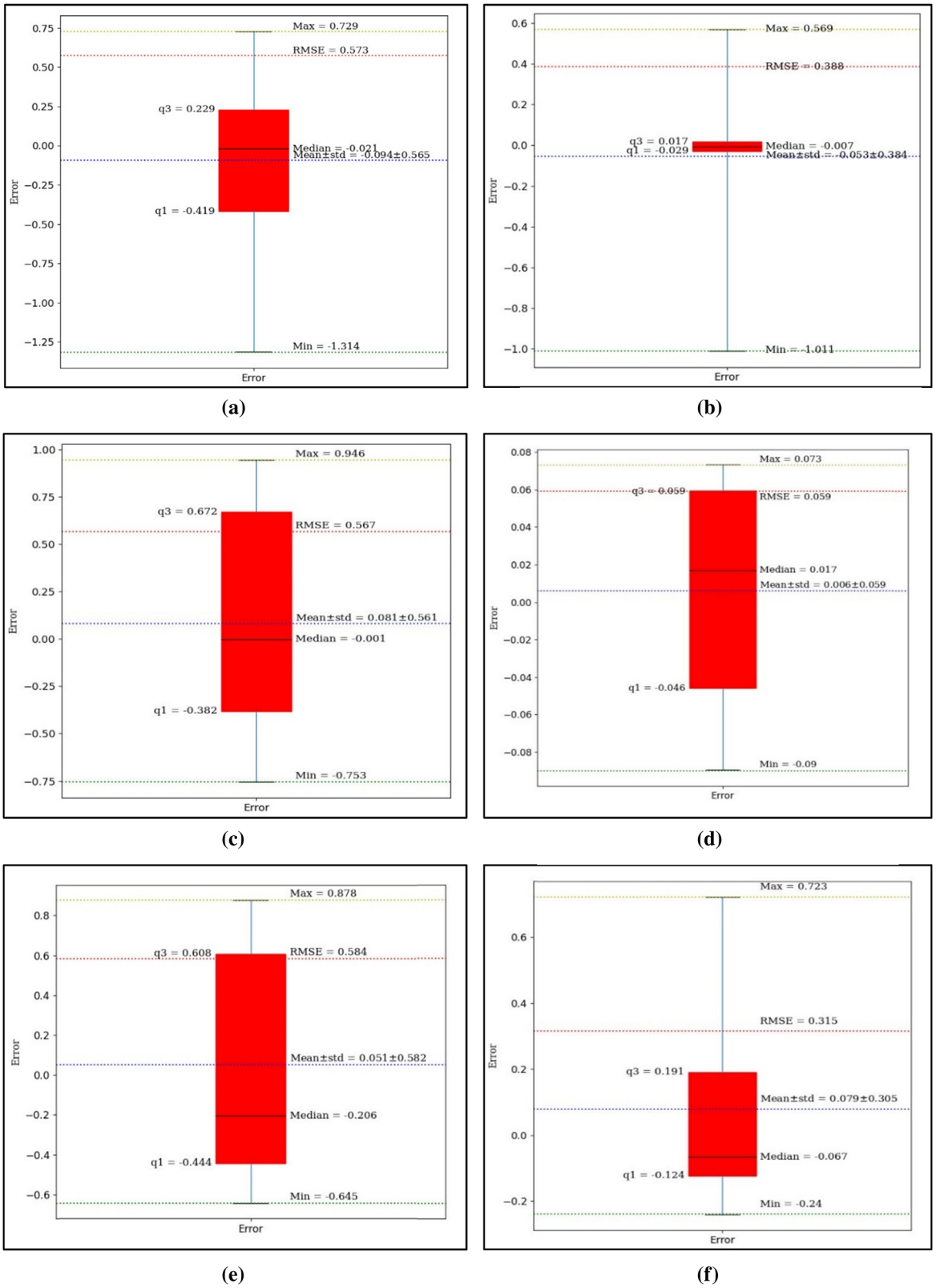

Figure 10: The statistical results of the check process using the Smart Map Plugin (OK) method and the IDW method, for the main road to exit Al-Sadr City, and for three measurement periods, morning, noon and evening. (a) Check IDW morning, (b) Check Smart Map (OK) morning, (c) Check IDW noon, (d) Check Smart Map (OK) noon, (e) Check IDW evening, and (f) Check Smart Map (OK) evening.

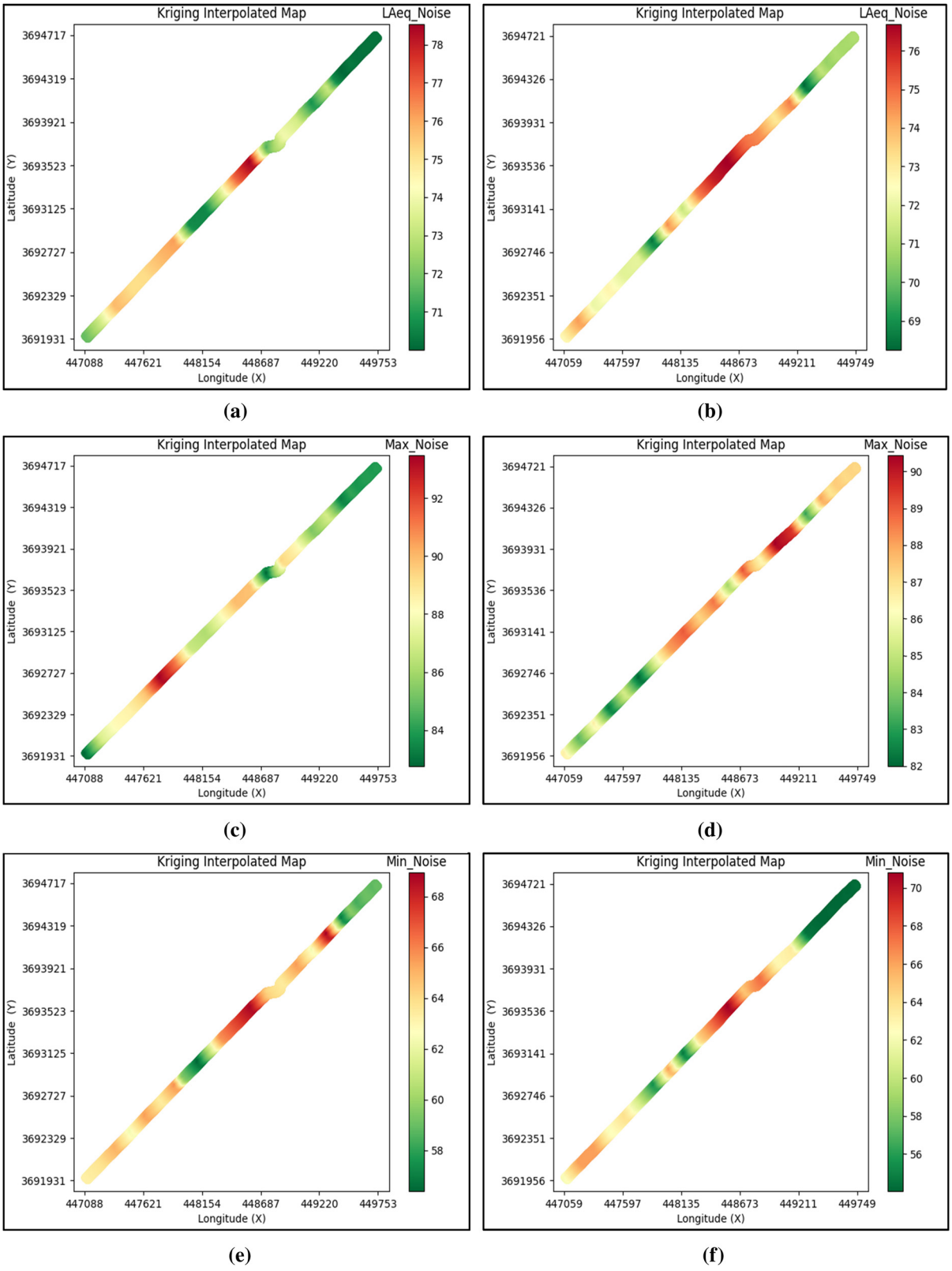

Figure 11: The resulting interpolation maps using Smart Map Plugin (OK) for the noise values of LAeq, Max, Min for the main road to enter and exit from Al-Sadr City at the morning. (a) Enter Main Road Smart Map Morning LAeq, (b) Exit Main Road Smart Map Morning LAeq, (c) Enter Main Road Smart Map Morning Max, (d) Exit Main Road Smart Map Morning Max, (e) Enter Main Road Smart Map Morning Min, and (f) Exit Main Road Smart Map Morning Min.

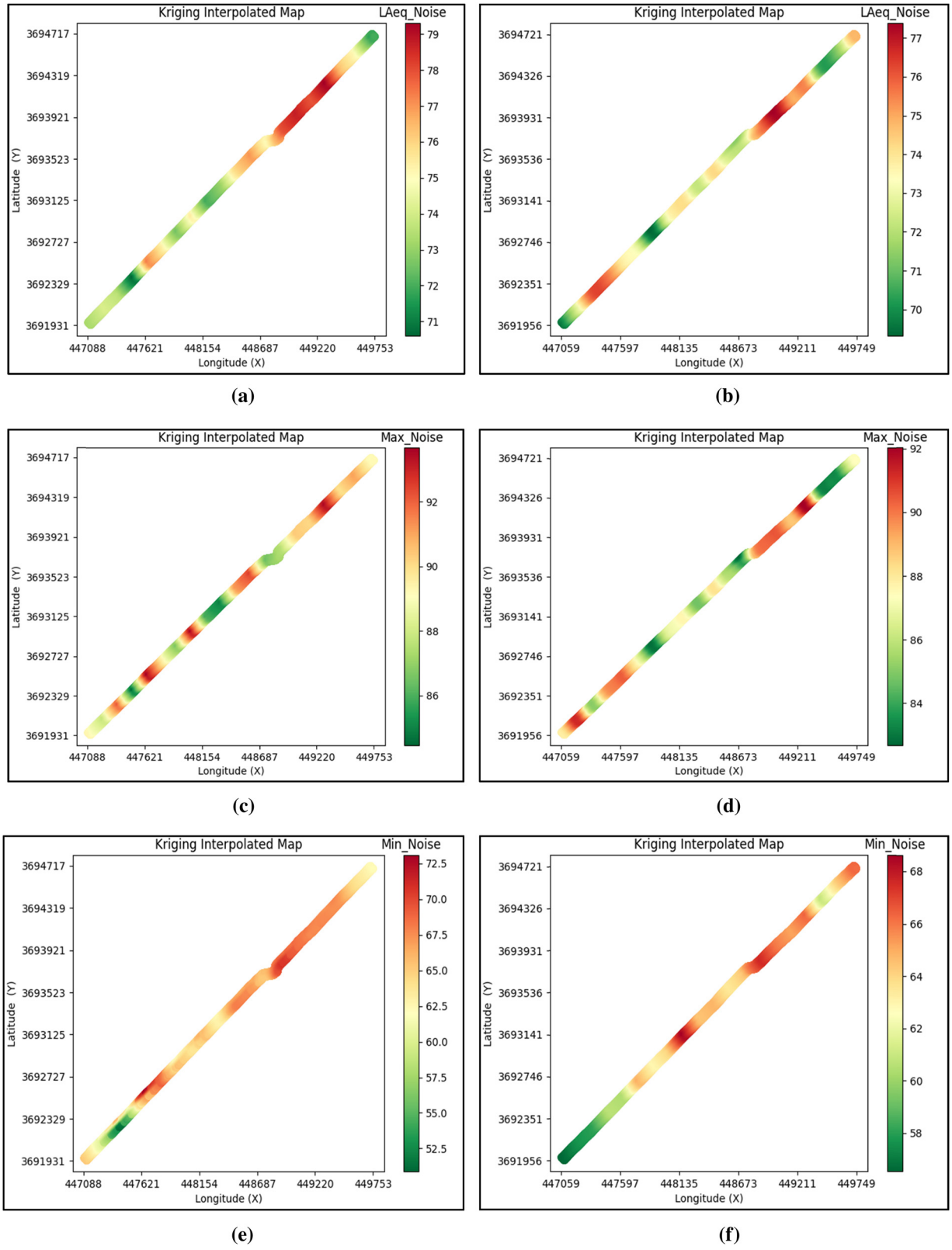

Figure 12: The resulting interpolation maps using Smart Map Plugin (OK) for the noise values of LAeq, Max, Min for the main road to enter and exit from Al-Sadr City at the noon. (a) Enter Main Road Smart Map Noon LAeq, (b) Exit Main Road Smart Map Noon LAeq, (c) Enter Main Road Smart Map Noon Max, (d) Exit Main Road Smart Map Noon Max, (e) Enter Main Road Smart Map Noon Min, and (f) Exit Main Road Smart Map Noon Min.

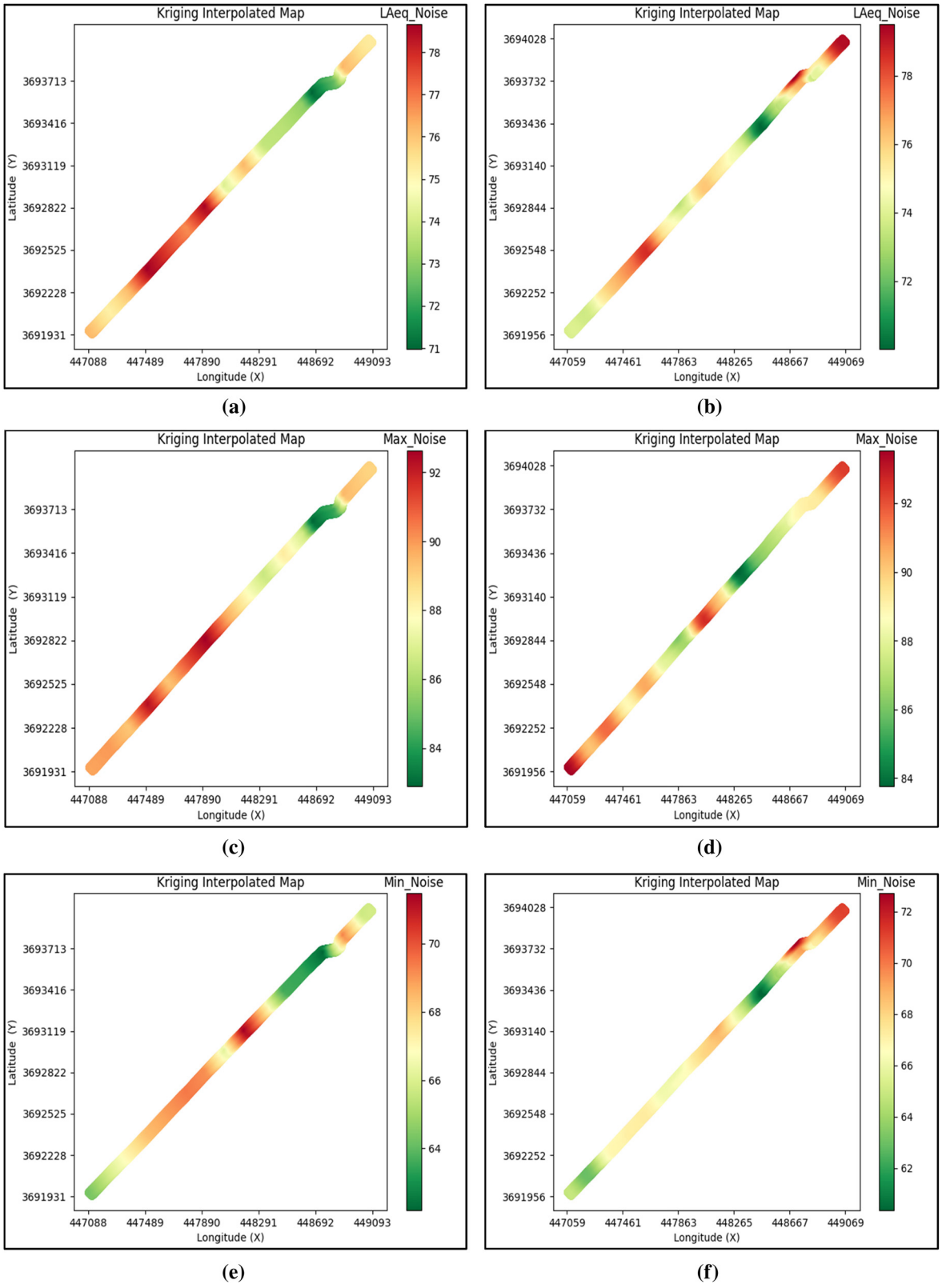

Figure 13: The resulting interpolation maps using Smart Map Plugin (OK) for the noise values of LAeq, Max, Min for the main road to enter and exit from Al-Sadr City at the evening. (a) Enter Main Road Smart Map Evening LAeq, (b) Exit Main Road Smart Map Evening LAeq, (c) Enter Main Road Smart Map Evening Max, (d) Exit Main Road Smart Map Evening Max, (e) Enter Main Road Smart Map Evening Min, and (f) Exit Main Road Smart Map Evening Min.

Table 4: The highest measured noise values and the lowest measured noise values during the three measurement periods for the main road of entry and exit from Al-Sadr City

Measurement time	Unit	Highest value (LAeq)	Highest value (Max)	Lowest value (Min)
Enter road morning	dB	78.536	93.478	53.306
Enter road noon	dB	79.308	93.674	58.24
Enter road evening	dB	78.66	92.624	62.19
Exit road morning	dB	76.688	90.44	54.042
Exit road noon	dB	77.484	91.936	56.544
Exit road evening	dB	79.002	93.41	70.978

noise levels in these areas should not exceed 50–70 dB during the daytime and 40–65 dB at night. However, the results showed that the actual noise levels measured along the main entry and exit roads of Al-Sadr city passing through these areas exceeded the allowable national limits. The highest noise values of LAeq and Max and the lowest noise values of Min for the three measurement periods in the morning, afternoon, and evening are presented in Table 4.

The study concludes that the Smart Map Plugin (OK) provides flexibility and ease of use in the initialization and modification of the appropriate semi-variogram model, which is used in the surface interpolation process to conduct an interactive investigation of the spatial behavior of noise phenomenon. Furthermore, this article highlights that the user is not restricted to using the OK method, which is available within GIS or QGIS software and lacks the capabilities of the Smart Map Plugin (OK). Additionally, the Smart Map Plugin provides the Moran's I spatial correlation index, facilitating the verification of spatial correlation among measured noise points. When Moran's I is high, OK performs better than IDW, as evidenced by the test results. Furthermore, after conducting a test using the measured LAeq noise values for the entry and exit roads of Sadr City, it was concluded that the Smart Map Plugin (OK) had the best performance and gave a lower RMSE than IDW for the three measurement periods. Additionally, the Plugin is also flexible, allowing the user to make modifications to its code. For example, the Plugin's code was modified to change the color gradient of the map indicator from red to green to logically match high and low noise level values.

Acknowledgments: The authors thank the Surveying Techniques Engineering Department, Technical College, Middle Technical University, and the Mustansiriyah University Engineering College, Highway and Transportation Dept. for supporting this research.

Funding information: The authors received no specific funding for this work.

Author contributions: We confirm that the three authors actively contributed to the realization and design of the current work, as well as to all data collection, analysis, and interpretation of its results to achieve the basic research goals, in addition to drafting the manuscript as required, and we bear responsibility for the various work paragraphs.

Conflict of interest: The authors declare that there is no conflict of interest to report regarding the present study.

References

[1] Garg N. Environmental noise control: The Indian perspective in an international context. Cham, Switzerland: Springer Nature; 2022.
[2] Ersoy S, Waqar T. Autonomous vehicle and smart traffic. IntechOpen; 2020. Available from: http://dx.doi.org/10.5772/intechopen.81968.
[3] Adulaimi AAA, Pradhan B, Chakraborty S, Alamri A. Traffic noise modelling using land use regression model based on machine learning, statistical regression and GIS. Energies. 2021;14(16):5095.
[4] Kwafe FE, Avwiri GO. Noise pollution mapping of Woji Town, Port Harcourt. Int J Innovative Res Sci Eng Technol. 2022 Jan;11(1):592–600.
[5] Mac Domhnaill C, Douglas O, Lyons S, Murphy E, Nolan A. Road traffic noise and cognitive function in older adults: A cross-sectional investigation of The Irish Longitudinal Study on Ageing. BMC Public Health. 2021;21(1):1–14.
[6] Mann S, Singh G. Traffic noise monitoring and modelling—an overview. Environ Sci Pollut Res Int. 2022;29:1–12.
[7] Münzel T, Sørensen M, Daiber A. Transportation noise pollution and cardiovascular disease. Nat Rev Cardiol. 2021;18(9):619–36.
[8] Hassanien AE, Bhattacharyya S, Chakrabati S, Bhattacharya A, Dutta S. Emerging technologies in data mining and information security: Proceedings of IEMIS 2020. Singapore: Springer; 2020.
[9] Bies DA, Hansen CH, Howard CQ. Engineering noise control. Boca Raton (FL), USA: CRC Press; 2017.
[10] Licitra G, editor. Noise mapping in the EU: Models and procedures. Boca Raton (FL), USA: CRC Press; 2012.
[11] Department of Science and Technology, Ministry of Science and Technology, Government of India, Government of India. Interpolation Techniques Using QGIS [Accessed August 7, 2022]. https://dst-iget.in/.
[12] Şorea I, Stoleriu CC, Ursu A. Road traffic noise modeling. Case study: Vaslui Town, North-Eastern Romania. In: Şerban G, Croitoru A, Tudose

T, Horváth C, Bătinaş R, Holbâcă I, editors. Air and Water–Components of the Environment Conference Proceedings; 2019 Mar 22–24; Cluj-Napoca, Romania. p. 375084.
[13] Harman BI, Koseoglu H, Yigit CO. Performance evaluation of IDW, Kriging and multiquadric interpolation methods in producing noise mapping: A case study at the city of Isparta, Turkey. App Acoust. 2016;112:147–57.
[14] Pereira GW, Valente DSM, de Queiroz DM, Santos NT, Fernandes-Filho EI. Soil mapping for precision agriculture using support vector machines combined with inverse distance weighting. Precis Agric. 2022;23:1–16.
[15] Huang T, Chan TC, Huang YJ, Pan WC. The association between noise exposure and metabolic syndrome: A longitudinal cohort study in Taiwan. Int J Environ Res Public Health. 2020;17(12):4236.
[16] Aumond P, Can A, Mallet V, De Coensel B, Ribeiro C, Botteldooren D, et al. Kriging-based spatial interpolation from measurements for sound level mapping in urban areas. J Acoust Soc Am. 2018;143(5):2847–57.
[17] Segura Garcia J, Pérez Solano JJ, Cobos Serrano M, Navarro Camba EA, Felici Castell S, Soriano Asensi A, et al. Spatial statistical analysis of urban noise data from a WASN gathered by an IoT system: Application to a small city. Appl Sci. 2016;6(12):380.
[18] Taghizadeh-Mehrjardi R, Zare M, Zare S. Mapping of noise pollution by different interpolation methods in recovery section of Ghandi telecommunication Cables Company. J Occup Health Epidemiol. 2013;2:1–11.
[19] Fredy Alejandro GL, Marco Andres GL, Nestor Yezid RR. Spatial-temporal assessment and mapping of the air quality and noise pollution in a sub-area local environment inside the center of a Latin American Megacity: Universidad Nacional de Colombia-Bogotá Campus. Asian J Atmos Environ. 2018;12(3):232–43.
[20] Hasan Sojib R, Basak SB, Seddique AA, Bodiuzzaman M, Tabassum S. The status of noise pollution of Mymensingh City, Bangladesh: A GIS-based noise mapping. IOSR J Environ Sci Toxicol Food Technol. 2021;15:7–15.
[21] Thanh B, Hanh N. Mapping and distribution of noise using IDW interpolation algorithm in Thuan An city, Binh Duong province. Thu Dau Mot Univ J Sci. 2021;3(4):64–76.
[22] Karakuş CB, Yıldız S. Evaluation of noise pollution level from traffic for Sivas city using GIS-based noise indexes. Cumhuriyet Sci J. 2020;41(1):176–84.
[23] Ameen MH, Jumaah HJ, Kalantar B, Ueda N, Halin AA, Tais AS, et al. Evaluation of $PM_{2.5}$ particulate matter and noise pollution in Tikrit university based on GIS and statistical modeling. Sustainability. 2021;13(17):9571.
[24] Ali SM, Hama AR, Ali YM. A study of Land zoning in the base of traffic noise pollution levels using ArcGIS: Kirkuk City as a case study. Al-Khwarizmi Eng J. 2017;13(4):137–51.
[25] Oyedepo SO, Adeyemi GA, Olawole OC, Ohijeagbon OI, Fagbemi OK, Solomon R, et al. GIS–based method for assessment and mapping of noise pollution in Ota metropolis, Nigeria. Methods X. 2019;6:447–57.
[26] Akintunde EA, Bayei JY, Akintunde JA. Noise level mapping in University of Jos, Nigeria. GeoJournal. 2020;87:1–13.
[27] Anitha SelvaSofia SD, Divyabharathi S, Backya P, Swetha S, Balamithra A. GIS based assessment and mapping of noise pollution in Coimbatore district. Int J Innov Technol Explor Eng. May 2019;8(1):3435–41.
[28] Arokoyu SB, Emenike GC, Atasi LT. Assessment of road junctions' noise levels in Yenagoa metropolis, Nigeria using geographic information systems. Nat Sci. 2016;14(3):82–96.
[29] Benarieb S, Farhi A. QGIS free GIS software: An opportunity for the management of municipalities in Algeria Case of Biskra municipality, Poster. International Symposium on Applied Geoinformatics (ISAG-2019); 2019 Nov 7–9; Istanbul, Turkey.
[30] Chiedu S, Agbalagba E, Avwiri G. Noise pollution assessment of SELECTED junctions in Warri metropolis and its environs. Int J Innovative Environ Stud Res. 2021;9:27–39.
[31] Kumar V, Ahirwar AV, Prasad AD. Noise mapping during deepawali festival in Raipur City of Chhattisgarh, India. Eco Env Cons. 2022;28:979–83.
[32] Ghetta M, Puddu G, Cavallini P. AniMove: A Free and Open-source Framework for the Analysis of Animal Movements with QGIS, Poster. XII Congresso Italiano Di Teriologia; 2022 Jun 8–11; Cogne, Italy.
[33] Pereira GW, Valente DSM, Queiroz DMD, Costa ALDF, Coelho MM, Grift T. Smart-Map: An open-source QGIS plugin for digital mapping using machine learning techniques and ordinary kriging. Agronomy. 2022;12(6):1350.
[34] Gustavowillam. 4.-Interpolation-using-Ordinary-Kriging GitHub. April 16, 2023. https://tinyurl.com/2mbacecx.
[35] GeoStat-framework/PyKrige: Kriging toolkit for Python GitHub. Nov 15, 2022. https://github.com/GeoStat-Framework/PyKrige.
[36] Kriging Variogram Model. Nov 16, 2022. https://tinyurl.com/48m8ptwr.
[37] Graser A, Mearns B, Mandel A, Ferrero VO, Bruy A. QGIS: Becoming a GIS power user. Birmingham, UK: Packt Publishing Ltd; 2017.
[38] Johnston K, Ver Hoef JM, Krivoruchko K, Lucas N. Using ArcGIS geostatistical analyst. Vol. 380. Redlands: Esri; 2001.
[39] Chang KT. Introduction to geographic information systems. 9th ed. New York (NY), USA: McGraw-Hill Education; 2018.
[40] An overview of the interpolation toolset—ArcMap Pro documentation; Nov 30, 2022. https://pro.arcgis.com/en/pro-app/latest/tool-reference/spatial-analyst/an-overview-of-the-interpolation-tools.htm.
[41] Gao J. Fundamentals of spatial analysis and modelling. Boca Raton (FL), USA: CRC Press; 2022.
[42] Li J, Heap AD. Spatial interpolation methods applied in the environmental sciences: A review. Environ Modell Softw. 2014;53:173–89.
[43] Burrough PA, Goodchild MF, McDonnell RA, Switzer P, Worboys M. Principles of geographical information systems. Oxford, UK: Oxford University Press; 1998.
[44] Chen S, Wang Z. Noise mapping in an urban environment: Comparing GIS-based Spatial modelling and parametric approaches. J Digit Landscape Archit. 2020;5:122–9.
[45] How IDW works—ArcGIS Pro | Documentation; Nov 28, 2022. https://pro.arcgis.com/en/pro-app/latest/tool-reference/spatial-analyst/how-idw-works.htm.
[46] Li J, Heap AD. A review of spatial interpolation methods for environmental scientists. Canberra, Australia: Geoscience Australia; 2008.
[47] Spatial Analysis (Interpolation) — QGIS Documentation; Nov 25, 2022. https://docs.qgis.org/latest/en/docs/gentle_gis_introduction/spatial_analysis_interpolation.html.
[48] Mitas L, Mitasova H. Spatial interpolation. In: Longley P, Goodchild MF, Maguire DJ, Rhind DW, editors. Geographical information systems: Principles, techniques, management and applications. Hoboken (NJ), USA: Wiley; 1999.
[49] How Kriging works—ArcGIS Pro | Documentation; Nov 20, 2022. https://pro.arcgis.com/en/pro-app/latest/tool-reference/3d-analyst/how-kriging-works.htm.